1999

Metal and Oxygen Ion Transport during Ionic Conduction in Amorphous Anodic Oxide Films

Mei-Hui Wang
Iowa State University

Kurt R. Hebert
Iowa State University, krhebert@iastate.edu

Metal and Oxygen Ion Transport during Ionic Conduction in Amorphous Anodic Oxide Films

Abstract
A mathematical model was developed for ionic conduction in amorphous oxide films. The model is based on a hypothesized "defect cluster" mechanism in which both metal and oxygen ions are involved in transport. Defect clusters are created by inward displacement of oxygen ions around an oxygen vacancy-like defect in response to the vacancy's electric field. Metal ions are assumed to migrate easily in the gap between the first and second layer of oxygen ions around the vacancy. The model includes the polarization of the conductive gap in the applied electric field, the exchange of mobile metal ions in the cluster with stationary metal ions in the surrounding oxide, and space charge generated in the film by clusters and oxide nonstoichiometry. The rate-limiting step is the jump of the oxygen vacancy in the cluster. It was found that polarization of the cluster leads to a stoichiometric excess of metal ions in the cluster and that this excess produces a net transport of metal ions due to the motion of the cluster. The metal ion transport number was found to increase with electric field and to depend on the dielectric constant and cluster size. The field dependence follows that found experimentally. The calculated transport numbers are in quantitative agreement with experimental values for tantalum, niobium, and tungsten oxide but smaller than experimental values for aluminum oxide. The field coefficient in the high-field-conduction-rate expression is also predicted and agrees with experimental values to within 10%.

Disciplines
Chemical Engineering

Comments
This article is from *Journal of the Electrochemical Society* 146 (1999): 3741–3749, doi:10.1149/1.1392543. Posted with permission.

Journal of The Electrochemical Society, **146** (10) 3741-3749 (1999)
S0013-4651(98)09-078-8 CCC: $7.00 © The Electrochemical Society, Inc.

Metal and Oxygen Ion Transport during Ionic Conduction in Amorphous Anodic Oxide Films

Mei-Hui Wang[a] and Kurt R. Hebert*

Department of Chemical Engineering, Iowa State University, Ames, Iowa 50011, USA

A mathematical model was developed for ionic conduction in amorphous oxide films. The model is based on a hypothesized "defect cluster" mechanism in which both metal and oxygen ions are involved in transport. Defect clusters are created by inward displacement of oxygen ions around an oxygen vacancy-like defect in response to the vacancy's electric field. Metal ions are assumed to migrate easily in the gap between the first and second layer of oxygen ions around the vacancy. The model includes the polarization of the conductive gap in the applied electric field, the exchange of mobile metal ions in the cluster with stationary metal ions in the surrounding oxide, and space charge generated in the film by clusters and oxide nonstoichiometry. The rate-limiting step is the jump of the oxygen vacancy in the cluster. It was found that polarization of the cluster leads to a stoichiometric excess of metal ions in the cluster and that this excess produces a net transport of metal ions due to the motion of the cluster. The metal ion transport number was found to increase with electric field and to depend on the dielectric constant and cluster size. The field dependence follows that found experimentally. The calculated transport numbers are in quantitative agreement with experimental values for tantalum, niobium, and tungsten oxide but smaller than experimental values for aluminum oxide. The field coefficient in the high-field-conduction-rate expression is also predicted and agrees with experimental values to within 10%.

Manuscript submitted September 24, 1998; revised manuscript received May 7, 1999.

Anodic oxidation of valve metals in solutions which do not dissolve the oxide produces compact, nonporous oxide films which find use in dielectric applications. These anodic oxides include the films on aluminum, tantalum, tungsten, niobium, zirconium, and titanium,[1] the first four of which have amorphous structures.[2] Transport processes in anodic films have been extensively investigated experimentally. The anodic oxides are electronic insulators; during ionic conduction, the current density is proportional to $\exp(BE)$, in which E is the electric field in the film. The field coefficient B is approximately 5 cm/MV for all these systems.[1] The contributions of metal *vs.* oxygen ions to conduction have been studied by depositing immobile chemical species onto the films as markers.[2,3] The fraction of current carried by metal ions is denoted by t_M, the metal ion transport number. t_M is found to vary from 0.1 to 0.5 in the various systems[2] and to increase with electric field.[4,5] The mechanisms of ionic mass transport have been investigated using tracers, usually O^{18} isotopes for studying oxygen transport[6,7] and bilayer metal films to study metal ion transport.[6,8,9] Oxygen transport occurs via exchange between transported oxygen ions and those constituting the film. For crystalline oxides, this exchange would result from vacancy or exchange interstitial transport, although such a distinction is less meaningful in amorphous materials. In the case of metal ion transport, the available measurements suggest that exchange between transported and constituent ions also occurs, although there may be a contribution from interstitial-like transport as well.

Models for conduction in amorphous oxide films have evolved over time to include new concepts derived from experimental results. The earliest ion-conduction models for anodic films assumed that the current was carried exclusively by metal ions, via interstitial or vacancy-type defects.[6,10,11] This assumption was shown to be erroneous by the later marker studies of amorphous anodic films. These models take the rate-limiting step in conduction to be a jump of an ion into an interstitial site or vacancy, either within the oxide or at the interface. They yield an exponential current-field relation in which the field coefficient is related to the jump distance. While the form of the conduction law agrees with experiment, the calculated jump distance is found to be significantly larger than the average oxygen-oxygen distance.[12] More recently, detailed defect-conduction models have been developed for crystalline oxide films, for example, those on passive metals such as iron. These models include features such as interface reactions with the metal and the solution, defect equilibria in the oxide, and space-charge effects, which are also relevant for amorphous anodic films.[13,14] One of them, Macdonald's point-defect model, has also been applied to conduction in amorphous films.[13] However, it does not yield a high-field conduction law, and only oxygen ions contribute to film growth.

Fromhold pointed out that the comparable magnitude of metal and oxygen transport numbers is an important distinguishing feature for conduction in amorphous *vs.* crystalline films.[15] He argued that if transport occurred through independent metal and oxygen defects, the variability of the activation energies of motion of these defects would dictate that the transport of only one type of defect should predominate at a given temperature. In this case, the measured metal transport number would be either zero or one. For this reason, the comparable metal and oxygen transport rates in amorphous oxides suggests a cooperative mechanism for ion migration, as originally proposed by Pringle.[16] A number of authors have discussed transport in these films in terms of such cooperative mechanisms.[2,15,17-19] Cooperative transport is thought to arise from the amorphous structure of the anodic films, since in crystalline films, metal and oxygen transport numbers are not of comparable magnitude.

As pointed out by Despic and Parkhutik,[20] while it seems important to incorporate the features of the amorphous oxide structure in quantitative transport models, few efforts have done so.[21,22] The cooperative transport processes cited previously were described, for the most part, in qualitative terms. Pringle originally proposed that both metal and oxygen ions participate in the elementary transport event, during which the oxide structure locally loses its rigidity; details of this event were not specified, nor were transport numbers calculated.[16] Fromhold suggested that the cooperative transport event involves place exchange of metal and oxygen ions,[15] and calculated the transport number directly from the stoichiometry of the place exchange event, assuming that only these events contribute to charge transport. The calculated transport numbers agreed with experimental values only when several ions were involved in the place exchange. Fromhold's calculation did not consider, for example, the effect of the transported charged defects on the local electric field in the film, and he did not offer a rate expression for charge transport. Mott proposed that local excitations may be possible in amorphous oxide films involving on the order of 10 ions, in which, for a time on the order of 1 ps, the ions vibrate with a liquid-like amplitude about their positions.[18] During this brief time, liquid-type transport is possible within this "liquid-like cluster," causing both metal or oxygen ions to migrate

* Electrochemical Society Active Member.
[a] Present address: Industrial Technology Research Institute, Hsinchu, Taiwan.

S0013-4651(98)09-078-8 CCC: $7.00 © The Electrochemical Society, Inc.

in the field with roughly equal probability. Other investigators have mentioned the place-exchange or liquid-like cluster mechanisms in discussing their experimental results,[5,19] but these ideas have not yet been developed further as quantitative transport models.

In this paper, a cooperative ion conduction mechanism for an amorphous oxide film is described and then developed as a mathematical transport model for the film. The model is used to predict mass transport of metal and oxygen ions during steady-state anodic growth of amorphous oxide films on aluminum, tantalum, niobium, and tungsten. These predictions are compared with experimental measurements, with particular regard to the transport number, its dependence on electric field, and the field coefficient *B*. The model views the elementary process of conduction as the jump of an oxygen ion into a vacancy-like site, as suggested by the tracer experiments. However, metal ions in the amorphous oxide near the vacancy are transported along with the vacancy. The calculations show that this hypothesis results in quantitatively reasonable predictions for conduction phenomena. The model is limited to steady-state oxide growth and does not consider transients produced by current or potential modulation.[23,24] Additionally, the influence of mechanical strain energy in the film on conduction is not included in the model.[25]

Mathematical Model

As described previously, conduction of ionic charge in the oxide film in the model involves jumps of oxygen ions into vacancy-like sites. In the following, the oxygen ion vacancy together with its associated mobile metal ions is referred to as a "defect cluster."

General description of the defect cluster.—On the basis of X-ray diffraction measurements of anodic aluminum oxide, the local arrangement of oxygen ions is considered to be similar to a close packing, with metal ions located in some of the interstitial sites between the oxygen ions.[26,27] At the vacancy, the absence of an oxygen ion leads to a net charge of 2*e* around the vacant site. The resulting electric field causes surrounding oxygen ions to move inward toward the vacancy until the electric force is balanced by strong short-range repulsion. To a first approximation, the electric field around the vacancy can be viewed as arising from a point charge at the vacancy

$$E_r = \frac{2e}{4\pi\epsilon r^2} \qquad [1]$$

where r is the distance from the vacancy. This relation suggests that for an oxide with $\epsilon = 10\epsilon_0$, the electric field on the second layer of oxygen ions around the vacancy ($r = 6$ Å) is about 25% of the field on the first layer ($r = 3$ Å). In fact, Grimes and Catlow, on the basis of molecular-scale computer simulations of crystalline oxides, indicate that the attenuation of the displacive force is even more rapid than $1/r^2$ due to electrostatic screening by the first layer of oxygen ions.[28] Hence, one may expect that the inward displacement of the oxygen ions in the first layer is greater than that of the second layer. A gap would then be produced between the first and second layers of oxygen ions. If the gap is of sufficient width, the activation energy required for metal ions to migrate between interstitial sites within the gap is reduced significantly. Therefore, under an external electric field, the metal ions would migrate downfield and polarize the region around the vacancy. Conductive gaps are expected to be much more probable in amorphous compared to crystalline oxides, since crystalline films have a smaller volume per oxygen ion. Thus, the inward displacement around the vacancy would be less likely to provide a gap of sufficient width for metal ion migration.

Figure 1 illustrates a layer of oxygen ions including an oxygen vacancy (A or B). The vacancy is enclosed by three more oxygen ions on top of the layer and three more below the layer. The figure depicts the inward displacements of six oxygen ions in the layer around the vacancy. The cross section of a conductive gap is shown surrounding the 12 nearest oxygen neighbors of the vacancy. The vacancy, together with the conductive gap, constitutes the defect cluster. The conductive gap moves with the vacancy as the vacancy hops from site to site, as shown in the figure. The presence of defect

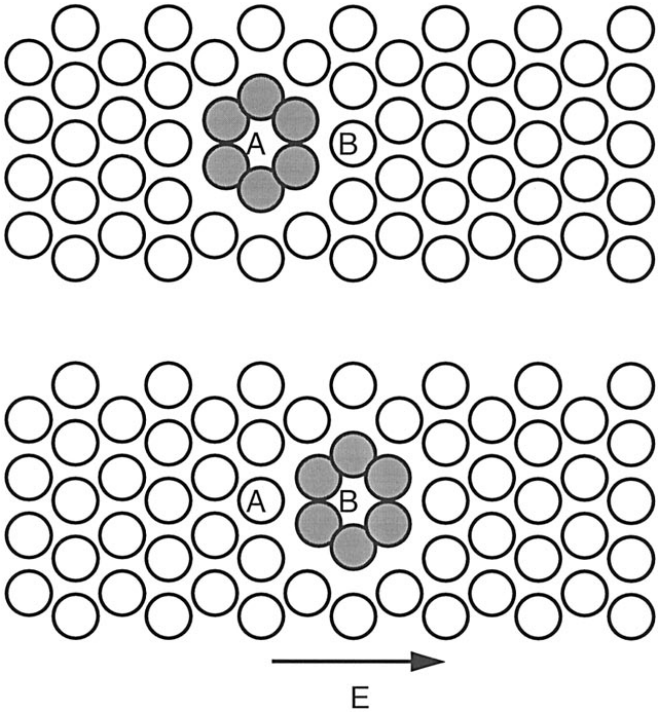

Figure 1. The displacement of a vacancy-centered cluster as the vacancy hops from site A to site B. Circles represent oxygen ions, and shaded circles are those neighboring the vacancy.

clusters is postulated in the model, and the calculations described in this section explore the consequences of clusters for ionic transport. The calculations show that some of the metal ions in the gap are carried along with the vacancy in this hopping motion so that vacancy migration leads to transport of both metal and oxygen ions.

Electrical polarization within the defect cluster.—The distribution of the mobile metal ions in the conductive gap can be viewed in terms of the electrical polarization of the gap under a uniform field. The polarization is established by the free movement of metal ions in the gap. This motion of metal ions is "liquid-like" in the sense of Mott's idea; [18] however, in the present model, it is only the metal ions in the gap which behave in this way, and not both metal and oxygen ions as Mott suggested.

For the purpose of calculating the metal ion distribution, the gap is modeled as a conductive spherical shell in a dielectric material. The choice of the spherical shape simplifies the application of the boundary conditions at the surface of the cluster. The electrostatic potential outside the sphere obeys Laplace's equation

$$\nabla^2\phi = 0 \qquad [2]$$

This equation, which assumes that the space charge in the oxide is zero, is meant to apply to the atomic-scale region immediately around the defect cluster. This region is assumed to be small enough so that it does not include other defect clusters or charged defects. The potential within the conductive spherical shell is uniform after the polarization, since any nonzero potential gradient would cause charge to flow. Thus, one boundary condition is obtained by setting the potential at r_0, the outer radius of the sphere, to zero. The uniform potential in the conductive region also requires $\partial\phi/\partial r|_{r=r_0} = 0$. In addition, any net charge must migrate to the surface at r_0. According to Gauss's law

$$-\oint \left.\frac{\partial\phi}{\partial r}\right|_{r=r_0} dS = \frac{q_0}{\epsilon} \qquad [3]$$

where q_0 is the total charge of the cluster. For simplicity, it is assumed that the entire charge of the cluster, including that of the vacancy, is included in q_0. In a more sophisticated model, a portion of the vacan-

S0013-4651(98)09-078-8 CCC: $7.00 © The Electrochemical Society, Inc.

cy charge would be considered to reside at the vacancy and would not be assigned to the conductive gap. The final boundary condition relates the potential far away from the sphere to the applied field E

$$\phi(r \to \infty) = -Er \cos\theta + \text{constant} \quad [4]$$

With these three boundary conditions, the solution of Eq. 2 is

$$\phi = \frac{q_0}{4\pi\epsilon}\left(\frac{1}{r} - \frac{1}{r_0}\right) + Er\left(\frac{r_0^3}{r^3} - 1\right)\cos\theta \quad [5]$$

The constant in Eq. 4 was chosen so that the potential at r_0 is zero. The induced surface charge density, determined from Eq. 5 using Gauss's law, is

$$\sigma = -\epsilon\left.\frac{\partial\phi}{\partial r}\right|_{r=r_0} = \frac{q_0}{4\pi r_0^2} + 3\epsilon E\cos\theta \quad [6]$$

Since only metal ions are considered responsible for the polarization, the transport of metal ions can be derived from the surface charge distribution. From Eq. 6, one can see that the surface charge density with $\theta < \pi/2$ is more positive than that with $\theta > \pi/2$; thus, metal ions are found preferentially on the downfield side of the spherical shell, as expected.

Calculations of ion transport in the oxide films requires a value for r_0, the radius of the cluster. r_0 is related to the distribution of the interstitial sites in the gap, which have either octahedral or tetrahedral coordination to their neighboring oxygen ions. For a "close packed" arrangement of oxygen ions, the distance between the center of the vacancy and that of a tetrahedral site in the gap is 1.17 $a_{O\text{-}O}$, where $a_{O\text{-}O}$ is the distance between the centers of two neighboring oxygen ions. The distance between the center of the vacancy and that of an octahedral site in the gap is 1.23 $a_{O\text{-}O}$. Because the average O-O distance for the amorphous anodic oxides considered here is about 2.98 Å,[29] the average distance between the center of the oxygen vacancy and an interstitial site in the gap is $1.20 \times 2.98 = 3.57$ Å. This distance is used later for the value of r_0. Note that this calculation assumes that the geometric arrangement of oxygen ions is the same as a close-packed crystalline oxide, but the spacing between oxygen ions is derived from the amorphous film density.

The calculation of the distribution of metal ions in the gap accounts for their electrostatic energy due to interactions with the external field, the charge density in the gap, and the surrounding dielectric. The interactions do not include short-range repulsion between the metal ions or electrostatic repulsion between the metal ions and the vacancy. These factors would cause a stoichiometric excess of metal ions on the downfield side of the gap to be less energetically favorable and would thus decrease the downfield charge from that indicated by Eq. 6. On the other hand, repulsion between the gap metal ions and the vacancy is attenuated by screening provided by the first layer of oxygen ions. Also, the extent of interstitial-interstitial repulsion between the downfield metal ions in the gap depends on their concentration; it is shown in the Discussion section that the predicted concentration is increased by only about 20% compared to stoichiometry. For these reasons, the effects of these replusive interactions on the calculated polarization may be relatively small.

Hopping of the cluster.—Transport of the defect cluster is accomplished by the jump of an oxygen ion immediately outside the cluster into the cluster. The cluster can allow the addition of another oxygen ion due to the void space offered by the vacancy. The jump is promoted by the electric field outside the cluster. One possible mechanism for the jump is that the hopping oxygen pushes one of its neighboring oxygen ions in the cluster into the vacancy site in order to make room for its addition at the cluster boundary. As a result of the jump, the vacancy is relocated to the site from which the oxygen jumped, as shown in Fig. 1.

If the top of the energy barrier for the transfer of the oxygen ion into the cluster is located at the cluster boundary, the jump frequency depends on the free energy change associated with the displacement of the oxygen ion from its lattice site to the cluster boundary. However, it is considered likely that metal ions neighboring the jumping oxygen ion can migrate at the same time.[2,15,17-19] One then needs to consider the displacements of both metal and oxygen ions to account for the free energy change.

This simultaneous motion of metal and oxygen ions was considered by Fromhold,[15] who viewed it as the rotation of a group having composition MO_p. If p is $|z_M/z_O|$, MO_p is a stoichiometric unit of the oxide and the rotation is a stoichiometric rotation. The argument that stoichiometric rotations should be favored is that since each MO_p unit is electrically neutral, it constitutes an electric dipole. During the rotation of such a unit, the electrostatic energy of the oxide increases due to interactions with the dipole moments of surrounding stoichiometric units. If, however, the rotation were nonstoichiometric, the electrostatic energy would also increase due to charge-charge interactions as metal ions are separated from their stoichiometric units. The energy cost of this separation would be large, since it would involve displacing metal ions from their closest oxygen ion neighbors. Therefore, the stoichiometric rotation is considered to be most energetically favorable and it is taken as the elementary process of oxygen transport.

Figure 2 illustrates the rotation of the stoichiometric unit MO (*i.e.*, for $p = 1$) in which the metal ion moves from r_0 to r_1 and the oxygen ion moves from r_1 to r_0. With the presence of a potential difference $\Delta\phi$ between r_0 and r_1, the change in electrical potential energy associated with the rotation is $(z_M\text{-}z_O)e\Delta\phi$, or $-2z_Oe\Delta\phi$. The free energy change due to the rotation is then

$$\Delta F = \Delta F^\circ - 2z_Oe\Delta\phi \quad [7]$$

where ΔF° is the free energy change with a uniform potential. This result holds for any oxide stoichiometry, since the net charge associated with the rotating metal ions would always be two. The jump frequency is therefore written as

$$\nu_j = \nu\exp\left(-\frac{\Delta F^o}{kT}\right)\exp\left(\frac{2z_oe\Delta\phi}{kT}\right) = \nu_0\exp\left(\frac{2z_oe\Delta\phi}{kT}\right) \quad [8]$$

Since the potential difference $\Delta\phi$ varies in the θ direction according to Eq. 5, the jump frequency for an oxygen ion neighboring the cluster depends on its location on the cluster surface. To determine which oxygen around the cluster is likely to jump, ν_j/ν_0 from Eq. 8 was calculated as a function of θ. $\Delta\phi$ is $\phi(r_0) - \phi(r_0 + {}^1/_2a_{M\text{–}O})$ where $a_{M\text{–}O}$ is the M–O bond length, approximately 1.7 Å. The net cluster charge, q_0 in Eq. 5, for the purposes of this calculation is taken to be the vacancy charge, $2e$, although it can be larger (as discussed later). For the case of aluminum oxide, with a dielectric constant of 10 and applied field of 7.3 MV/cm, the plot of $\log_{10}(\nu_j/\nu_0)$ *vs.* θ is shown in Fig. 3. According to the figure, the jump frequency decreases dramatically with θ, indicating that only the oxygen ion located closest to $\theta = 0$ has a significant probability of jumping into the vacancy cluster.

After the oxygen ion jumps, the center of the cluster moves downfield, for example, from site A to site B in Fig. 1. The conductive gap also moves with the cluster. Hence, metal ions which occupied the upfield portion of the old gap around site A are no longer part of the new gap around site B. These metal ions are now trapped in interstitial sites between oxygen ions, effectively having lost their mobility as a result of the jump. Metal ions on the downfield side of the gap around site A remain mobile, since they are incorporated into the new cluster around site B. In order to treat quantitatively metal ion transport, it is necessary to estimate the fraction of metal ions in the old conductive gap which incorporate into the new cluster. For this purpose, the overlap between the old location and the new location of the cluster can be approximated as the overlap of two spheres of the same size, as shown in Fig. 4. The fraction of the surface area of the old cluster overlapped by the new cluster is

$$\frac{A_1}{4\pi r_0^2} = \frac{1 - \cos\theta_1}{2} \quad [9]$$

S0013-4651(98)09-078-8 CCC: $7.00 © The Electrochemical Society, Inc.

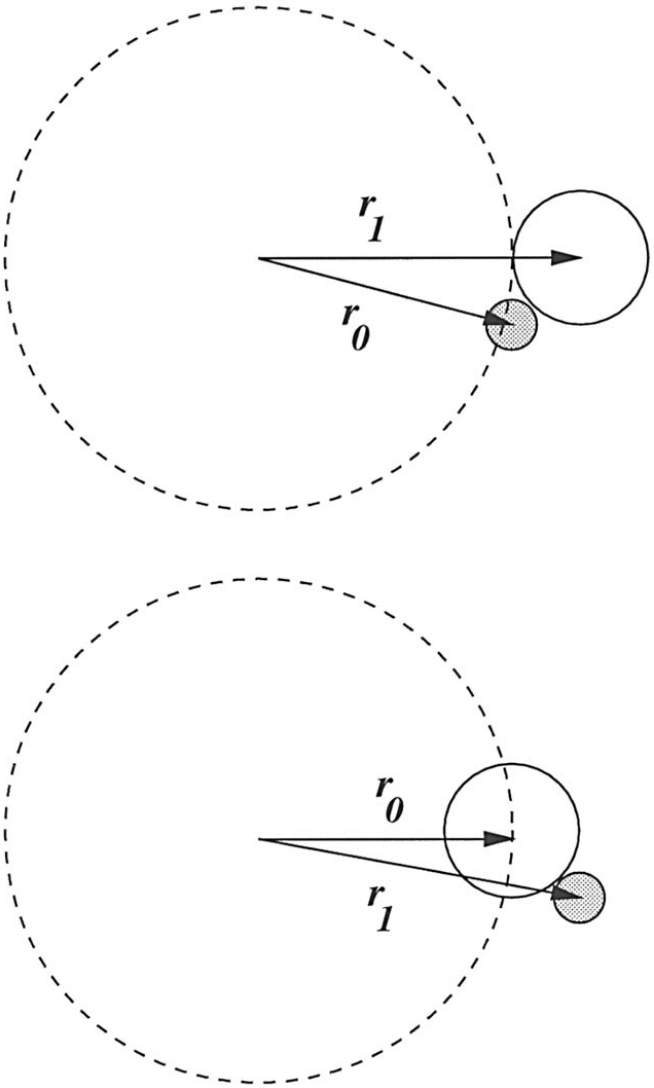

Figure 2. Rotation of the stoichiometric unit consisting of one oxygen ion (open circle) and one metal ion (shaded circle) in an oxide of formula MO. The large dashed circle represents the cluster boundary.

where A_1 is the overlapped area and θ_1 is the overlap angle shown in the figure. By integrating the surface charge on A_1 according to Eq. 6, one obtains the total surface charge which remains in the cluster after the vacancy jump

$$q_1 = \frac{q_0}{2}(1 - \cos\theta_1) + 3\pi\epsilon E r_0^2[1 - (\cos\theta_1)^2] \qquad [10]$$

The charge on the upfield side of the gap which is left behind after the jump is q_0-q_1 or

$$q_2 = \frac{q_0}{2}(1 + \cos\theta_1) - 3\pi\epsilon E r_0^2[1 - (\cos\theta_1)^2] \qquad [11]$$

It is clear that as a result of repeated jumps of the oxygen vacancy, immobile space charge is generated in the oxide film. The value of the overlap angle in Eq. 9-11, θ_1, is determined by the radii of the two spheres and the distance between the centers. With a radius r_0 of 3.57 Å and a center-center distance of 5.27 Å, θ_1 is found to be 0.25 π.

Mass-transport equations.—In this section the description of the jumping process given in the last section is formulated as a mass-transport model which can be used to calculate the rates of metal and oxygen ion transport across the film. The model equations are written as if the transport process were macroscopic in nature and the oxide film were a dilute solution of charged defects. Transport in

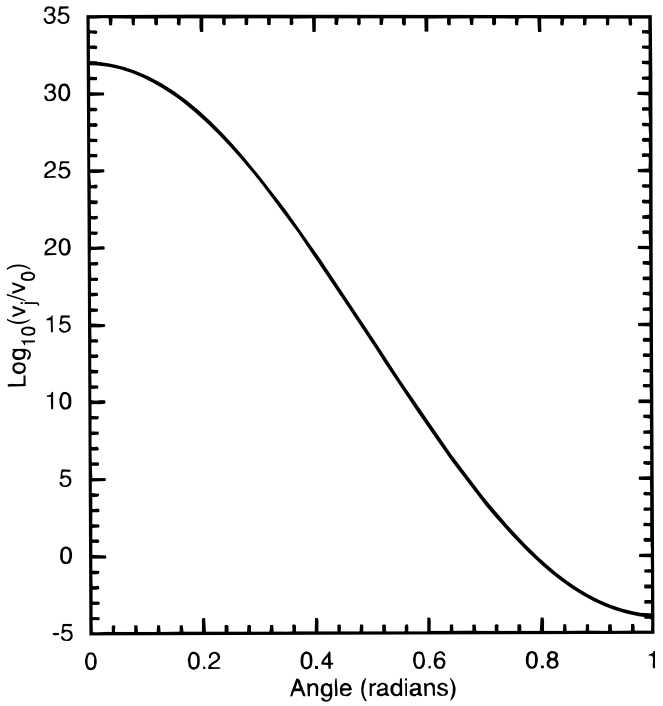

Figure 3. The variation of the normalized jump frequency, ν_j/ν_0, with angular position around the cluster. $\theta = 0$ refers to the extreme downfield point on the cluster surface.

ionic thin films was first modeled in this way by Wagner,[30] and more recently by Chao *et al.*[13] and Battaglia and Newman.[14] This pseudo-macroscopic approach results in relatively simple model equations, while still incorporating important physical constraints due to electrostatics and mass conservation. Its use is therefore appropriate for the present purpose of exploring the implications of defect clusters for mass transport.

As described previously, the jump of the oxygen vacancy causes immobile space charge to be created on the upfield side of the clus-

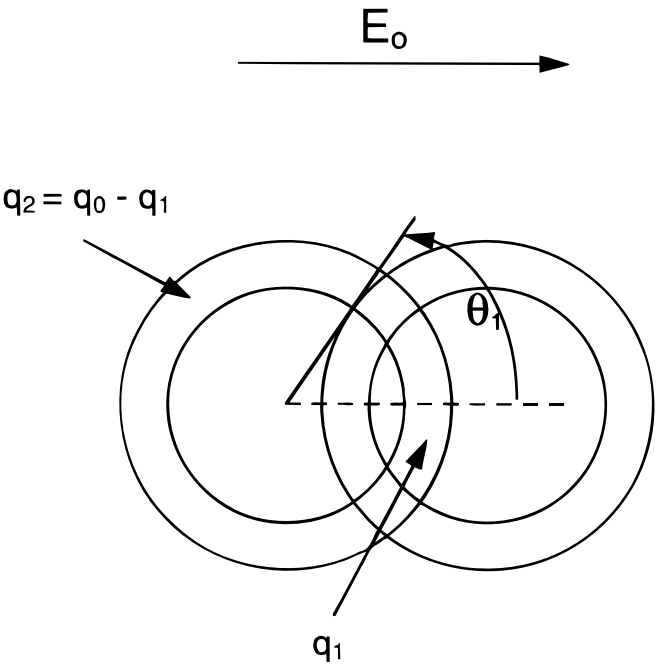

Figure 4. Overlap between the locations of a cluster before and after the vacancy jump.

S0013-4651(98)09-078-8 CCC: $7.00 © The Electrochemical Society, Inc.

ter. Thus, the overall conduction process produces a background space-charge density distributed through the oxide film. The presence of this space charge may affect the electric field in the oxide which drives the hopping of the clusters. Hence, the background space-charge density from immobile metal ions must be considered in order to predict the rates of ionic transport. When a cluster moves through the oxide, two processes occur which contribute to this space charge. The first, as already described, is the formation of new space charge on the upfield side of the cluster. The rate of this process per unit volume of oxide is

$$c_v N_A \frac{v_v}{a}(q_2 + \beta z_o e) \quad [12]$$

The second term in parentheses reflects that when a new oxygen ion jumps into the central vacancy, a fraction of its charge should be left behind as immobile space charge. This fraction is estimated to be β, defined as $(A_0 - A_1)/A_0$ or $(1 + \cos\theta_1)/2$. In Eq. 12, the jump frequency is expressed as the velocity of vacancy motion, v_v, divided by the jump distance *a*. The second process contributing to the space-charge density is the incorporation of immobile space charge into the cluster, on its downfield side, as it moves to occupy new volumes of oxide. The rate of incorporation per volume is

$$c_v \frac{v_v}{a} \rho_{eM} \beta \bar{V}_0 \quad [13]$$

The net rate of production of space charge is the difference between Eq. 12 and 13.

The equation for space-charge formation, as well as the other model equations, is written in terms of chemical rather than electrical variables so that mass-transport rates can be identified more clearly. In terms of chemical variables, the immobile space-charge density outside the clusters, ρ_{eM}, is expressed as a relative stoichiometric excess of metal ions, c'_M

$$\rho_{eM} = z_M F c'_M = z_M F\left(c_M + \frac{z_O}{z_M} c_O\right) \quad [14]$$

Recall that according to the model, lattice oxygen ions in the region outside the clusters are immobile so that c_O, the concentration of these ions, is fixed and any variation of c'_M is attributable to a variation of c_M. Similarly, the cluster charge, q_0, can be written in terms of a relative stoichiometric excess of metal ions, n'_M, as $q_0 = z_M e n'_M - z_O e$. The balance on immobile space charge is then

$$\frac{\partial c'_M}{\partial t} = \beta c_v \frac{v_v}{a}\left(n'_M - c'_M \bar{V}_0 - \frac{6\pi\gamma\epsilon E r_0^2}{z_M e}\right) \quad [15]$$

where Eq. 10 has been used to relate q_1 to q_0. γ is defined as $1 - \cos\theta_1$. This equation has the standard form of differential mole balances, including accumulation and reaction terms, but since the metal ions are immobile, it has no term representing the transport flux.

The transport model also includes mole balances on oxygen vacancies and on metal ions incorporated into clusters. The oxygen vacancy balance is

$$\frac{\partial c_v}{\partial t} = -\frac{\partial (c_v v_v)}{\partial x} \quad [16]$$

The spatial variation of the concentrations and electric field is considered to be one-dimensional and depends only on *x*, the coordinate measured from the metal/film interface. The balance on mobile metal ions inside clusters is

$$\frac{\partial}{\partial t}\left[c_v(n'_M - c'_M \bar{V}_0)\right] = -\frac{\partial c'_M}{\partial t} - \frac{\partial}{\partial x}\left[c_v v_v (n'_M - c'_M \bar{V}_0)\right] \quad [17]$$

The term in square brackets on the left side is the concentration of mobile metal ions in clusters per unit volume of oxide. Note that $n'_M - c'_M \bar{V}_0$ gives the change of the local number of metal ions when a cluster arrives at a new site and that it thus yields the correct number of metal ions moving along with the cluster. Equations 16 and 17 are also written in the usual form of differential mole balance equations: the terms on the left sides represent accumulation of the species in question and the right sides contain terms representing the divergence of the transport flux of the species. The first term on the right side of Eq. 17 is the rate of incorporation of immobile metal ions into clusters, according to Eq. 15. Transport of vacancies is considered to occur only by electrical migration, according to the migration velocity v_v. The neglect of diffusion is supported by the oxygen tracer measurements of Pringle,[7] who anodized tantalum first in ^{16}O and then in ^{18}O, and found only a small diffusional mixing between the layers of oxide containing each isotope.

In addition, the model includes Poisson's equation, which relates the spatial variation of the electric field in the oxide to the net space-charge density

$$\epsilon \frac{\partial E}{\partial x} = \rho_e = -z_O F c_v + z_M F c_v n'_M + z_M F c'_M (1 - c_v \bar{V}_0) \quad [18]$$

This equation is meant to describe variations of the electric field over a length scale which is larger than the mean distance between charged defects in the film but smaller than the film thickness. This length scale is significantly larger than that on which Laplace's equation (Eq. 2) is solved for the potential distribution around individual clusters. In the case of Eq. 2, it was appropriate to neglect space charge since the length scale of the region of interest is smaller than the mean distance between charged defects. Equation 18 does not account for electronic charge, since all the anodic oxide films under consideration are insulators; Di Quarto *et al*. report bandgap energies for aluminum, tantalum, tungsten, and niobium oxides to be 6.3, 3.95, 2.75, and 3.35 eV, respectively, measured using photocurrent spectroscopy.[31] With these bandgap energies essentially no electrons would be excited from the valence to the conduction band.

Finally, as mentioned previously, the vacancy velocity, v_v, is the product of the hopping frequency and the jump distance, *a*

$$v_v = a\nu_j = a\nu \exp\left(-\frac{\Delta F^o}{kT}\right) \exp\left(\frac{2 z_O e \Delta\phi}{kT}\right) \quad [19]$$

where $\Delta\phi$ is a function of *E* and q_0 according to Eq. 5.

Oxygen vacancies are formed at the metal/film interface by oxidation of metal atoms at a rate which is limited by the rate of vacancy removal by migration into the film. Hence, the concentration of vacancies at this interface is determined by the number of active sites at which oxidation occurs. According to Cabrera and Mott,[11] the active sites are kink sites on the metal surface. In the model, the number density of kink sites is considered to be constant during oxidation so that the vacancy concentration at the interface is a constant, c_{vo}. This boundary condition is used in the integration of the model equations. The value of c_{vo} is unknown, but it should be much smaller than the concentration of lattice ions, which is on the order of 10^{-2} mol/cm^3. The effect of this parameter on the calculated results is considered in the Results section.

While Eq. 15-17 are written in transient form, it is shown in the Appendix that transient terms are not significant during film growth. In the following calculations, these terms are neglected and transport in the film is taken to be at steady state.

Results

Solution of the model equations at steady state.—The model consists of four equations, Eq. 15-18, with the independent variables c_v, c'_M, n'_M, and E. Equations 15-18 may be integrated at steady state to obtain

$$c_v v_v = c_1 \quad [20]$$

$$n'_M c'_M \bar{V}_0 = c_2 \quad [21]$$

$$E = \frac{z_M e}{6\pi\gamma\epsilon r_0^2} c_2 \quad [22]$$

S0013-4651(98)09-078-8 CCC: $7.00 © The Electrochemical Society, Inc.

where c_1 and c_2 are constants of integration. Equation 22 indicates that the electric field is constant and everywhere equal to E_o, the field at the interface. The constant electric field implies that the net space charge, ρ_e, is zero. Using Eq. 18, the cluster charge, q_0, can then be obtained

$$q_0 = z_M e n'_M - z_O e = (1 - c_v \bar{V}_0)(6\pi\gamma\epsilon r_0^2 E_0 - z_O e) \qquad [23]$$

Thus, q_0 is a function of c_v and E_o. Since the vacancy velocity, v_v, depends on q_0 and E, v_v can be considered to be a function of c_v and E_o. Equation 20 then implies that c_v is constant and everywhere equal to c_{vo}, the concentration at the metal/film interface. n'_M and c'_M can then be expressed in terms of the boundary conditions c_{vo} and E_o

$$n'_M = \frac{6\pi\gamma E_o \epsilon r_0^2}{z_M e}(1 - c_{vo}\bar{V}_0) + \frac{z_O}{z_M} c_{vo}\bar{V}_0 \qquad [24]$$

$$c'_M = \frac{z_O}{z_M} c_{vo} - \frac{6\pi\gamma\epsilon r_0^2}{z_M e} c_{vo} E_o \qquad [25]$$

At steady state, the electric field, the vacancy concentration, the immobilized metal ion concentration, and the number of metal ions per cluster are all found to be uniform in the oxide. The space-charge density due to clusters exactly cancels the background space-charge density associated with the stoichiometric deficiency of metal ions in the oxide so that the net space-charge density is zero. This result agrees with the experimental finding that the current/field relationship does not depend on film thickness.[32] It is emphasized that zero net space charge is a result of the model calculations which apply only at steady state and that it is a consequence of the model equations rather than an assumption built into them.

Calculations of transport number and field coefficient.—Calculations of the defect concentrations, metal ion transport number, and field coefficient are presented in this section for the ranges of the electric field typically found during growth of various oxide films. The electric field ranges are usually narrow: for example, a range of fields from 7.3 to 8.1 MV/cm was considered for aluminum oxide. The values of some of the other parameters in the equations for the steady state are set to values which have been given before, *e.g.*, r_0 and r_1 are taken as 3.57 and 5.27 Å, respectively. θ_1 is 0.25π, from which β is 0.8536 and γ is 0.2929.

Calculated values of c'_M and q_0 with c_{vo} set to 10^{-4} mol/cm^3 are listed in Table I, along with the corresponding experimental range of applied fields and dielectric constant for each oxide. The results for aluminum oxide are plotted in Fig. 5 as an example. If a different value of c_{vo} were used, c'_M would change proportionally to c_{vo}, but q_0 would be independent of c_{vo} as long as c_{vo} remained smaller than 10^{-4} mol/cm^3. As shown in the figure, c'_M is negative, implying a stoichiometric deficiency of metal ions of about 0.13%. c'_M decreases linearly with the electric field while q_0 increases linearly with the field. These trends suggest that when E is increased, some metal ions are transferred into the cluster from the surrounding oxide due to the higher polarization. Thus, the polarization of clusters by the applied field causes them to absorb metal ions from the surrounding oxide so that clusters always carry a stoichiometric excess of metal ions. This excess provides the mechanism of metal ion transport by clusters. Also, both Table I and Fig. 5 indicate that within the given field ranges, the variations of c'_M and q_0 are both small. This result suggests that if the applied current were suddenly changed, the resulting adjustments in the defect concentrations would be very small, so perhaps the transient response of the field should be very rapid.

The transport number of metal ions can also be found from the model. The number of metal ions transported by the cluster is $n'_M - c'_M\bar{V}_0$. The charge carried by these metal ions is $z_M e(n'_M - c'_M\bar{V}_0)$. Of course, the cluster also carries one oxygen vacancy with a charge of $-z_O e$. The metal ion transport number, or the fraction of the cluster charge carried by the metal ions, is then found from Eq. 24 and 25

Table I. Calculated model results for various oxides: relative stoichiometric excess metal ion concentration c'_M, and cluster charge number q_0/e.

	ϵ/ϵ_0	E (MV/cm)	$-c'_M$ ($\times 10^{-5}$ mol/cm^3)	q_0/e
Al_2O_3	10.0[33]	7.3-8.1[33]	7.60-7.70	2.28-2.32
Ta_2O_5	23.2[34]	5.8-7.2[36]	5.04-5.29	2.52-2.65
Nb_2O_5	41.4[35]	3.5-5.0[37]	5.12-5.60	2.56-2.80
WO_3	41.7[38]	4.9-5.9[38]	4.65-4.92	2.80-2.96

$$t_M = \frac{6\pi\gamma E_o \epsilon r_0^2}{6\pi\gamma E_o \epsilon r_0^2 - z_O e} \qquad [26]$$

The transport number is then independent of the cluster concentration but depends on the electric field, permittivity, and cluster radius. Table II summarizes the calculated transport numbers of various metal oxides along with their dielectric constants and the experimental range of electric fields. Ranges of experimental values of transport numbers found at various current densities are listed for comparison. The calculated ranges of t_M overlap with the experimental ranges, except for the case of aluminum oxide for which the predicted values are somewhat smaller than the experimental ones. It is clear, however, that in all cases the model yields metal and oxygen transport numbers on the same order of magnitude, which can be regarded as an important point of agreement with experimental behavior.

Plots of calculated transport numbers *vs*. electric field are presented in Fig. 6. The figure demonstrates the model prediction that t_M increases with the field. As described in the Introduction, the experimental values of t_M for the oxides are also found to increase with current density in most cases. For example, Khalil and Leach reported t_M measurements for Ti, Zr, Ta, and Al, in each case for applied current densities of 6 and 50 mA/cm^2, and found that in each case the transport number increased with current by increments ranging from 0.02 to 0.09.[4] The implied slope dt_M/dE for Ta is 0.047 cm/MV compared to 0.029 cm/MV predicted by the model. Hence, in the

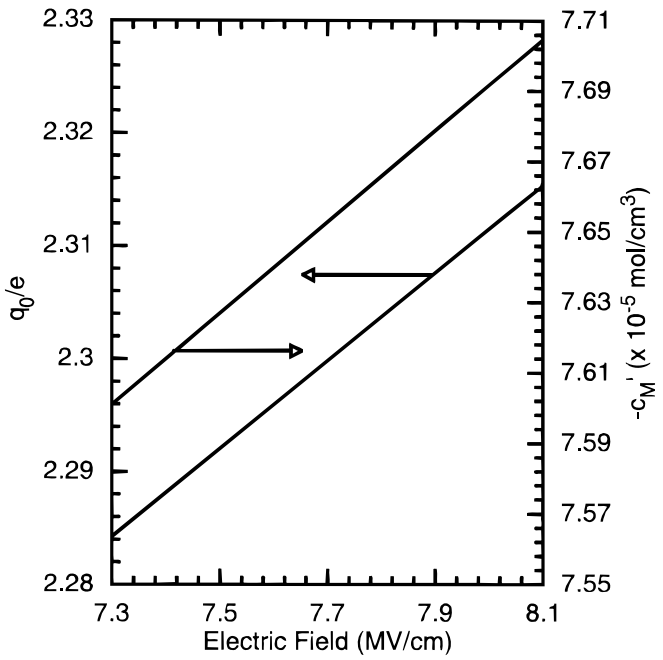

Figure 5. Relative stoichiometric deficiency of metal ions in the oxide film, $-c'_M$, and cluster charge number, q_0/e, as a function of electric field for the case of aluminum oxide with vacancy concentration, c_{vo}, set to 10^{-4} mol/cm^3.

S0013-4651(98)09-078-8 CCC: $7.00 © The Electrochemical Society, Inc.

Table II. Comparison of calculated and experimentally measured metal ion transport numbers, t_M, and experimentally measured field coefficient, B, for various amorphous oxides. The calculated field coefficient is the same for all oxides, 4.8 cm/MV. Ranges of values correspond to the range of electric fields.

	ϵ/ϵ_0	E (MV/cm)	t_M (Calculated)	t_M (Experimental)	B (cm/MV) (Experimental)
Al_2O_3	10.0[33]	7.3-8.1	0.12-0.14	0.40-0.45	4.7-5.0[33]
Ta_2O_5	23.2[34]	5.8-7.2	0.21-0.25	0.24-0.31	4.8[36]
Nb_2O_5	41.4[35]	3.5-5.0	0.22-0.29	0.22-0.33	6.4[37]
WO_3	41.7[38]	4.9-5.9	0.28-032	0.30-0.37	5.2[38]

case of Ta the model predicts a field dependence of t_M which is quantitatively comparable to the available experimental results. The results for Al are not compared, since Khalil and Leach report no difference in field for the two applied currents. It would be desirable to obtain experimental transport numbers over a wide range of fields in order to test the prediction from Eq. 26 that t_M approaches zero at low field and one at very high field. However, as noted before, the practical range of fields for high-field conduction is very small, and this comparison may not be possible.

The relation between the current density and electric field during oxide growth has been experimentally well-established for the various oxides. The model current density is

$$i = c_{v_0} a\nu(q_0 N_A - z_M F c'_M \bar{V}_0) \exp\left(-\frac{\Delta F^o}{kT}\right) \exp\left(\frac{2 z_O e \Delta\phi}{kT}\right) \quad [27]$$

The conduction current density was calculated for the four oxides over the experimental range of electric fields in Table II. Again, q_0 and $\Delta\phi$ are determined by the values of c_v and E. $c_{v_}$was set to 10^{-4} mol/cm^3 as before; with this value, the term $z_M F c'_M \bar{V}_0$ in Eq. 27 is negligible in comparison with q_0, and $c_v \bar{V}_0$ in Eq. 23 can be neglected as well. The parameter a was taken as 5.27 Å, ν as 10^{12} s^{-1}, [11] and $\Delta F°$ was adjusted so that the current density at the lowest value of E in the range agreed with the experimental current density. The resulting values of $\Delta F°$ were 2.56 for aluminum oxide, 1.87 for tantalum oxide, 1.35 for niobium oxide, and 1.01 eV for tungsten oxide. These free energy changes are considered to be reasonable, since $\Delta F°$ is expected to be on the order of magnitude of 1 eV. [11] However, $\Delta F°$ is not required for the determination of the field coefficient (B in the equation $i = Ae^{BE}$). The calculated and experimental conduction current density are plotted against the electric field in Fig. 7. The figure shows that the slopes (field coefficients) of all four model curves are nearly the same at 4.81(±0.02) cm/MV. There is good agreement with the experimental field coefficients, the values of which are listed in Table III.

Discussion

The metal ion transport numbers predicted by the model agree well with the experimental values, except in the case of aluminum oxide for which the calculated value is low. The predicted t_M would be greater if the cluster radius for aluminum oxide were larger than the assumed value of 3.57 Å, since according to Eq. 26, the transport number increases with the cluster radius. The clusters in aluminum oxide might in fact be larger than the assumed size because the aluminum ion is the smallest of the four metal ions under consideration: the radius of Al^{+3} ions with a coordination number of six is 0.54 Å, while those of Ta^{+5}, Nb^{+5}, and W^{+6} ions are 0.64, 0.64, and 0.60 Å, respectively.[39] For the relatively small aluminum ions, a small increase in the distance between oxygen neighbors can be sufficient for their easy migration. Therefore, aluminum ions may be mobile in the smaller gap between the second and third layers of oxygen ions around the vacancy. In this case, the outer boundary of the cluster

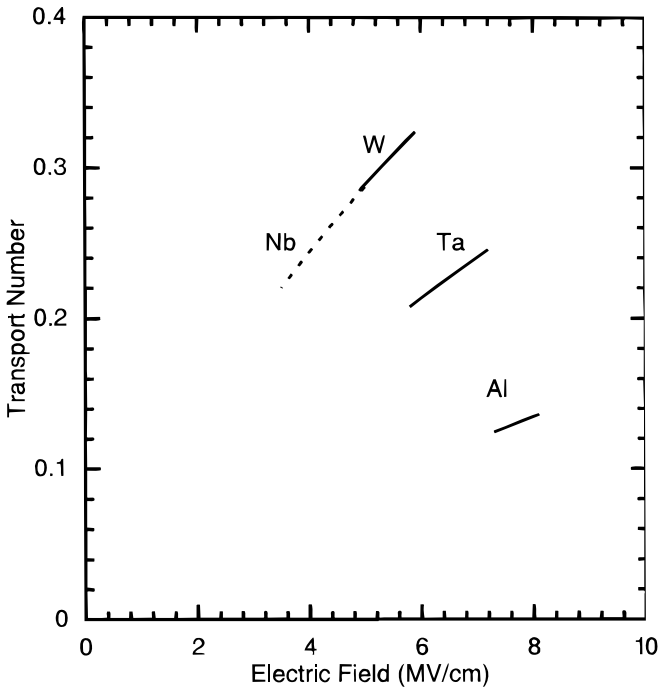

Figure 6. Metal ion transport number, t_M, *vs*. the electric field, E, oxides of four metals.

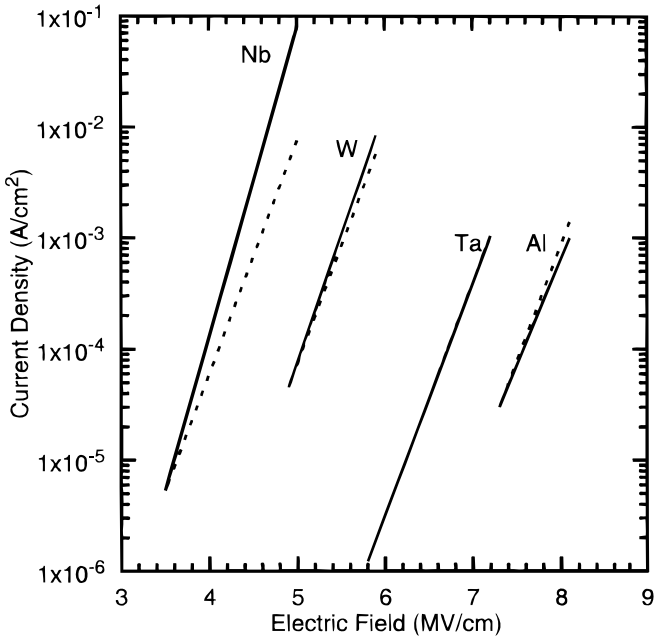

Figure 7. Conduction current density *vs*. electric field from the model and experimental data for oxides of four metals: (- - -) model predictions and (—) are experimental measurements for Al, [8] Ta, [11] Nb, [12] and W, [13] respectively. The jump free energy change, $\Delta F°$, was adjusted so the experimental and calculated curves agreed at the lowest current density in the range.

S0013-4651(98)09-078-8 CCC: $7.00 © The Electrochemical Society, Inc.

Table III. Calculated results for large defect clusters, with conductive gap between second and third layers of oxygen ions away from the vacancy (r_0 = 6.57 Å).

	$-c'_M$ ($\times 10^{-5}$ mol/cm^3)	q_0/e	t_M	B (cm/MV)
Al_2O_3	10.6-11.1	3.19-3.32	0.37-0.40	5.28
Ta_2O_5	8.31-9.43	4.16-4.73	0.52-0.58	5.31
Nb_2O_5	8.71-10.7	4.37-5.28	0.54-0.63	5.37
WO_3	8.88-10.0	5.34-6.02	0.63-0.67	5.35

would be at a radial distance of 6.57 Å from the vacancy center, corresponding to the distance of interstitial sites in the second gap from the vacancy center.

To demonstrate the effect of a larger assumed cluster size, model calculations were carried out for the case of a cluster radius of 6.57 Å. The larger value of r_0 required adjusting the parameter r_1 to 8.27 Å and θ_1 to 0.28π. The calculated results with these new parameters are given in Table III and can be compared with the results for the cluster radius of 3.57 Å in Tables I and II. The increase of q_0/e with r_0 indicates that larger clusters carry a larger number of metal ions; consequently, they have larger transport numbers. For aluminum, the transport numbers for the larger clusters are very close to the experimental values, while the calculated t_M values of other oxides are significantly larger than the experimental ones. Table III also indicates that the calculated field coefficient B is affected by the choice of a larger cluster size. Once again, the field coefficients of the four oxides are similar, and the average is 5.33 cm/MV. This value of B is close to 5.3 cm/MV, the average of the four experimental values, but it is not significantly different from the field coefficient of 4.8 cm/MV calculated for the smaller cluster. It can be concluded that the larger assumed cluster size yields quantitatively more realistic t_M and B results for aluminum oxide but that the corresponding predictions for the other oxides are less realistic compared to the case of the small cluster. As argued previously, a larger cluster in aluminum oxide might be consistent with the smaller size of the aluminum ion.

One potential source of error in the model calculations is the possible presence of short-range chemical and electrostatic repulsive forces between the metal ions on the downfield side of the gap which were not considered in the calculation of the metal ion distribution in the gap. These repulsive interactions might cause the stoichiometric excess of metal ions in interstitial sites on the downfield side of the cluster to be energetically unfavorable. As previously discussed, this excess is the origin of the coupled transport of metal and oxygen ions in the model, and thus the comparable metal and oxygen ion transport numbers. The importance of this repulsive force can only be judged through atomistic calculations including short-range interactions, which are beyond the scope of the present model. However, it can be pointed out that even considering the excess of metal ions expected on the downfield side of the gap, the number of metal ions is still significantly smaller than the number of interstitial sites the metal ions can occupy. It can be demonstrated through a simple calculation that the number of interstitial sites in the part of the gap corresponding to $-\theta_1 < \theta < \theta_1$ is at least three; the fractional stoichiometric occupancy of these sites is less than 1/3. [29] According to the simulation, the excess number of metal ions in the same portion of the gap is 0.20 in aluminum oxide, 0.18 in tantalum oxide, 0.18 in niobium oxide, and 0.20 in tungsten oxide. Thus, the occupancy of the downfield interstitial sites in the gap is increased by only about 20% compared to the stoichiometric occupancy. Also, even with the increased occupancy of these sites, the metal ions are surrounded by a number of vacant interstitial sites so that the repulsion between individual ions should not be too large.

Conclusions

A mathematical model has been developed for ionic conduction in amorphous anodic oxide films. In the model, current is carried by defect clusters created by inward displacement of oxygen ions around an oxygen vacancy in response to the vacancy's electric field. The model hypothesis is that this displacement creates a gap between the first and second layers of oxygen ions surrounding the vacancy, within which metal ions can migrate easily with little required activation energy. Calculations are presented which explore the implications of these conductive gaps for transport processes. It is found that polarization of the conductive gap in the applied electric field leads to an increased number of metal ions populating the gap compared to stoichiometry. The excess number of metal ions in clusters accounts for a net transport of metal ions due to the motion of the vacancy across the oxide film. Thus, oxygen and metal ion migration are coupled together and occur as part of the same process. Coupled transport of this kind is probably possible only in amorphous oxides, since the volume per oxygen ion may be large enough so that the additional oxygen-oxygen separation around the vacancy can lead to the formation of conductive gaps. In fact, comparable transport rates of metal and oxygen ions are found only in amorphous oxides.

According to the model, the metal ion transport number increases with electric field and also depends on the dielectric constant and the cluster size. The calculations yield metal transport numbers which are in quantitative agreement with experiment for tantalum, niobium, and tungsten oxide but smaller than experimental values for aluminum oxide. The field coefficient in the high-field conduction rate expression was also predicted and found to agree to within 10% with experimental values. This agreement depends on the involvement of both metal and oxygen ions in the elementary vacancy jump which causes the cluster to move. It was pointed out that increasing the cluster size for aluminum oxide would improve the agreement of the transport number with experiment; a somewhat larger cluster might be expected due to the relatively small aluminum ion. The model predicts that the metal transport number increases with electric field or current density.

The model embodies critical features of qualitative conduction mechanisms for anodic oxide films previously proposed by Fromhold and Mott,[15,18] which describe the cooperative roles of oxygen and metal ions in the conduction process. In particular, the conductive gap of the defect cluster corresponds to the "liquid-like cluster" proposed by Mott, and as in Fromhold's mechanism, the elementary process of conduction is viewed as the place exchange of metal and oxygen ions. The conductive gap around the vacancy is considered to be more probable than Mott's liquid-like cluster, since the free volume requirement for liquid-like metal ion conduction in the gap is much smaller than that for localized liquid-like conduction of both metal and oxygen ions. Furthermore, it is believed likely that the oxygen vacancy would "donate" sufficient free volume to make this gap conduction possible. Beyond these differences in the qualitative picture of conduction, the primary achievement of this model is that for the first time, these ideas have been expressed mathematically in terms of kinetic and transport equations. Thus, the model calculations are based on the kinetic ionic conduction expressions coupled to the constraining physical laws governing electrostatics and mass conservation of defects. All the quantitative predictions of the model are found to be quantitatively consistent with the experimental results for the four systems studied. These include the field coefficient in the conduction-current equation and the transport number and its dependence on the electric field. To the authors' knowledge, no other model for anodic conduction has demonstrated these predictive capabilities. The agreement with experimental phenomena suggests that some essential features of the defect-cluster concept may be realistic.

Acknowledgments

Financial support from the National Science Foundation (grant DMR 9307308) is gratefully acknowledged.

Iowa State University assisted in meeting the publication costs of this article.

S0013-4651(98)09-078-8 CCC: $7.00 © The Electrochemical Society, Inc.

Appendix

The purpose of this appendix is to show that transient effects in Eq. 15-17 are not significant during steady film growth. After transforming these equations to dimensionless variables, the magnitudes of the transient terms are compared to those of other terms in the equations. The dimensionless position, vacancy concentration, and time variables are

$$z = \frac{x - x_1(t)}{x_2(t) - x_1(t)} \qquad [A\text{-}1]$$

$$\theta_v = \frac{c_v}{c_{vo}} \qquad \tau = \frac{v_1^* t}{\delta^*} \qquad [A\text{-}2]$$

where $x_1(t)$ and $x_2(t)$ are the time-dependent positions of the metal/film and film/solution interfaces, respectively, v_1^* is a characteristic velocity of the metal/film interface, and δ^* is a characteristic film thickness. Equation A-1 converts the domain of the model to one where the boundaries are stationary. δ^*/v_1^* is the characteristic growth time of the film and thus, both τ and θ_v are on the order of unity. In dimensionless form, the vacancy concentration balance Eq. 16 becomes

$$\frac{\delta}{\delta^*}\frac{\partial \theta_v}{\partial \tau} = \frac{\partial}{\partial z}\left(\theta_v \frac{v_1}{v_1^*}(1 - z) + \theta_v \frac{v_2}{v_1^*} z - \theta_v \frac{v_v}{v_1^*}\right) \qquad [A\text{-}3]$$

where v_2 is the velocity of the film/solution interface. Since the metal and oxygen transport numbers are on the same order of magnitude, v_2/v_1^* is on the order of one. In fact, all terms in this equation should be on the order of one except for the last term on the right side. At the metal/film interface, $-c_O v_1 = c_v v_v$. Hence, v_v/v_1^* is on the order of c_o/c_{vo}, which is likely to be very large. Thus, for equality in the Eq. A-3 to hold, the derivative of $\partial(\theta_v v_v)/\partial z$ must be close to zero. This is equivalent to assuming that transport of oxygen vacancies is at steady state and neglecting the moving boundary. A similar transformation applied to Eq. 17 shows that transport of metal ions inside clusters is at steady state.

Finally, the balance on metal ions outside clusters, Eq. 15, is considered. With the introduction of dimensionless variables, it becomes

$$\frac{\partial \theta'_M}{\partial \tau} = \beta \frac{c_{vo}}{c'^*_M}\frac{v_v}{v_1^*}\frac{\delta^*}{a}\left(n'_M - c'_M \overline{V}_O - \frac{6\pi\gamma\epsilon E r_0^2}{z_M e}\right) \qquad [A\text{-}4]$$

where θ'_M is c'_M/c'^*_M, and c'^*_M is the characteristic excess metal ion concentration. The time derivative on the left side is on the order of one. c_{vo}/c'^*_M is not known, but it should be at least as large as one. However, since both v_v/v_1^* and δ^*/a are large, the factor multiplying the parentheses is a large number, and thus the term in parentheses must be very small in order for equality to be maintained. Again, this is equivalent to the assumption of steady state.

List of Symbols

A	empirical pre-exponential constant in high-field conduction expression, A/cm^2
A_0	surface area of cluster, cm^2
A_1	overlapped surface area between cluster before and after jump, cm^2
a	displacement of cluster center due to vacancy jump, cm
B	empirical electric field coefficient in high-field conduction expression, cm/MV
c_M	concentration of metal ions in oxide film, mol/cm^3
c'_M	relative stoichiometric excess concentration of metal ions in oxide outside clusters, mol/cm^3
c_O	concentration of oxygen ions in oxide film, mol/cm^3
c_v	concentration of oxygen vacancies, mol/cm^3
c_{vo}	concentration of oxygen vacancies at metal/film interface, mol/cm^3
E	electric field, MV/cm
E_o	electric field at metal/film interface, MV/cm
e	elementary electronic charge, 1.60×10^{-19} C
i	current density, A/cm^2
k	Boltzmann constant, 1.38×10^{-23} J/K
N_A	Avogadro's number, 6.02×10^{23} mol^{-1}
n'_M	stoichiometric excess number of metal ions inside cluster, dimensionless
q_0	total cluster charge, C
q_1	portion of cluster charge remaining in cluster after vacancy jump, C
q_2	portion of cluster charge immobilized in oxide after vacancy jump, C
r	radial coordinate measured from center of cluster, cm
r_i	inner radius of conductive gap, cm
r_0	outer radius of conductive gap (radius of cluster), cm
r_1	average radial coordinate of metal ions involved in stoichiometric rotation, cm
T	temperature, K
t	time, s
t_M	metal ion transport number, dimensionless
V_0	molar volume of clusters, cm^3/mol
v_v	oxygen vacancy migration velocity, cm/s
x	spatial coordinate in oxide, cm
z_M	charge number of metal ions, dimensionless
z_O	charge number of oxygen ions, dimensionless
ΔF	free energy change associated with vacancy jump, J/mol

Greek

β	dimensionless constant related to overlap of cluster before and after vacancy jump
ϵ	permittivity of oxide, C/V-cm
ϵ_0	permittivity of free space, 8.854×10^{-14} C/V-cm
ϕ	electrostatic potential in oxide (macroscopic potential), V
γ	dimensionless constant related to overlap of cluster before and after vacancy jump
ν, ν_0	preexponential jump frequencies, s^{-1}
ν_j	jump frequency in presence of electric field, s^{-1}
θ	angular coordinate around cluster, radians
θ_1	overlap angle between cluster before and after jump, radians
ρ_e	total space charge density in oxide, C/cm^3
ρ_{eM}	background space-charge density due to relative stoichiometric excess of metal ions, C/cm^3
σ	surface charge density of cluster, C/cm^2

References

1. L. Young, *Anodic Oxide Films*, Academic Press, London (1961).
2. J. P. S. Pringle, *Electrochim. Acta*, **25**, 1423 (1980).
3. J. A. Davies, B. Domeij, J. P. S. Pringle, and F. Brown, *J. Electrochem. Soc.*, **112**, 675 (1965).
4. N. Khalil and J. S. L. Leach, *Electrochim. Acta*, **31**, 1279 (1986).
5. G. E. Thompson, Y. Xu, P. Skeldon, K. Shimizu, S. H. Han, and G. C. Wood, *Philos. Mag. B*, **55**, 651 (1987).
6. G. Amsel and D. Samuel, *J. Phys. Chem. Solids*, **23**, 1707 (1962).
7. J. P. S. Pringle, *J. Electrochem. Soc.*, **120**, 1391 (1973).
8. J. Perrière, S. Rigo, and J. Siejka, *J. Electrochem. Soc.*, **125**, 1549 (1978).
9. J. Perrière, J. Siejka, and S. Rigo, *Corros. Sci.*, **20**, 91 (1980).
10. E. J. W. Verwey, *Physica*, **2**, 1059 (1935).
11. N. Cabrera and N. F. Mott, *Rep. Prog. Phys.*, **12**, 163 (1948-1949).
12. L. Young, *Anodic Oxide Films*, p. 19, Academic Press, London (1961).
13. C. Y. Chao, L. F. Lin, and D. D. Macdonald, *J. Electrochem. Soc.*, **128**, 1187 (1981).
14. V. Battaglia and J. Newman, *J. Electrochem. Soc.*, **142**, 1423 (1995).
15. A. T. Fromhold, Jr., *J. Electrochem. Soc.*, **127**, 411 (1980).
16. J. P. S. Pringle, *J. Electrochem. Soc.*, **120**, 398 (1973).
17. M. J. Dignam, in *Oxides and Oxide Films*, Vol. 1, J. Diggle, Editor, p. 190, Marcel Dekker, New York (1972).
18. N. F. Mott, *Philos. Mag. B*, **55**, 117 (1987).
19. I. Montero, B. Pelloie, J. Perrière, J. C. Pivin, and J. M. Albella, *J. Electrochem. Soc.*, **136**, 1869 (1989).
20. A. Despic and V. P. Parkhutik, in *Modern Aspects of Electrochemistry*, J. O'M. Bockris, R. E. White, and B. E. Conway, Editors, Vol. 20, p. 401, Plenum Press, New York (1989).
21. P. Winkel, C. A. Pistorius, and W. Ch. van Geel, *Philips Res. Repts.*, **13**, 277 (1958).
22. V. P. Parkhutik and V. I. Shershulskii, *J. Phys. D: Appl. Phys.*, **19**, 623 (1986).
23. D. F. Taylor and M. J. Dignam, *J. Electrochem. Soc.*, **120**, 1299 (1973).
24. L. Young and D. J. Smith, *J. Electrochem. Soc.*, **130**, 408 (1983).
25. J. L. Ord, *J. Electrochem. Soc.*, **127**, 2682 (1980).
26. Y. Oka, T. Takahashi, K. Okada, and S. Iwai, *J. Non-Cryst. Solids*, **30**, 349 (1979).
27. R. Manaila, A. Dévényi, and E. Candet, *Thin Solid Films*, **116**, 289 (1984).
28. R. W. Grimes and C. R. A. Catlow, *J. Am. Ceram. Soc.*, **73**, 3251 (1990).
29. M.-H. Wang, Ph.D. Thesis, Iowa State University, Ames (1998).
30. C. Wagner, *Z. Physik. Chem. B.*, **21**, 25 (1933).
31. F. Di Quarto, C. Sunseri, S Piazza, and M. C. Romano, *J. Phys. Chem. B*, **101**, 2519 (1997).
32. M. J. Dignam, in *Oxides and Oxide Films*, Vol. 1, J. Diggle, Editor, p. 190, Marcel Dekker, New York (1972).
33. K. Videm, *The Electrochemistry of Uniform Corrosion and Pitting of Aluminum*, Kjeller Report, p. 17, p. 24, Institute for Atomenergi, Kjeller, Norway (1974).
34. L. Young, *Anodic Oxide Films*, p. 93, Academic Press, London (1961).
35. L. Young, *Anodic Oxide Films*, p. 188, Academic Press, London (1961).
36. L. Young, *Trans. Faraday Soc.*, **50**, 153 (1954).
37. L. Young, *Trans. Faraday Soc.*, **52**, 502 (1956).
38. L. Young, *Anodic Oxide Films*, p. 272, Academic Press, London (1961).
39. F. Scordari, *Fundamentals of Crystallography*, C. Giacovazzo, Editor, p. 420, Oxford University Press, Oxford (1992).